Supplemental Materials

Molecular Biology of the Cell

Shen et al.

Legends for Supplemental Figures

FIGURE S1. Effects of Mff and Fis1 on organelle fission and Drp1 localization in *C. elegans*. (A) Quantification of fission defects in Fis1, Mff, Fis1 Mff and Drp1 mutant strains. Images of 40 or more cells per strain were classified as having mitochondria with fragmented, tubular or connected morphologies. Percentages for each class are shown. (B) Peroxisomes, detected with P_{hs}*::GFP::SKL*, are punctate in wildtype and Fis1 mutant animals and elongated in Mff and Drp1 mutants. (C) Effects of Ca-ionophores on mitochondrial morphology in wildtype, Drp1 Fis1, Mff and Fis1 Mff mutant strains. The two ionophores that were tested both induce fragmentation in Fis1 and Mff mutants showing that neither protein is essential for mitochondrial fission in *C. elegans*. The bar is 10 μm. (D) Controls showing the effectiveness of RNAi for mitochondrial fusion Dynamins (*eat-3* and *fzo-1*) and for the mitochondrial fission Dynamin (*drp-1*). RNAi for *eat-3* and *fzo-1* induces fragmented mitochondria, while RNAi for *drp-1* leads to highly connected mitochondria. The bar is 10 μm. (E) Quantification of epistasis experiments with Fis1 and Mff double mutants grown on e*at-3*, *fzo-1* and *drp-1* RNAi feeding bacteria. Images were classified as described for panel B. (F) CFP::DRP-1 (red) in spots on mitochondria. Mitochondria were labeled YFP::TOM70 (green). (G) Subcellular fractionation through differential centrifugation produced a supernatant with cytosolic proteins (S2) and a mitochondrial pellet (P2). SDS-PAGE gels were loaded with 1 volume equivalent of S2 and 10 volume equivalents of P2. Blots were probed for DRP-1, for MOMA-1 (mitochondria) and for Tubulin (cytosol). DRP-1 antibody detected a prominent band of the predicted size and some lower molecular weight breakdown products (absent from the *drp-1* deletion strain).

FIGURE S2. Fis1 dependence, gradual disappearance of mitochondrial marker and presence of Drp1 in LGG-1 aggregates. (A) Triple labeling with mitochondrial matrix targeted mls::mCherry (red), YFP::Tom70 (green) and CFP::LGG-1 (blue) in a Fis1 mutant animal treated with Paraquat and no recovery time. The images show that LGG-1 clusters contain mitochondria. The bar is 10 μm. (B) Enlargements of the aggregate in panel C. The bar is 5 μm. (C) Rescue experiment showing that ectopic expression of Fis1 with the *myo-3* promoter eliminates LGG-1 aggregates in a Fis1 double mutant. Mitochondria are labeled with YFP::TOM (green) and aggregates are labeled with CFP::LGG-1 (red). The bar is 5 μm. (D) Examples of LGG-1 aggregates at different times of recovery after a 1 hr treatment with Paraquat, showing that the YFP::TOM70 (green) gradually disappears from these aggregates. Aggregates are detected with LGG-1::CFP (red). The bar is 10 μm. (E) Examples of double labeling with CFP::DRP-1 (red) and YFP::LGG-1 (green) in wildtype and the Fis1 double

mutant. Worms were untreated (no drug), treated for 1 hr with Paraquat (1 hr PQ), or treated for 1 hr with Paraquat followed by 5 hr recovery on plates without drug (1 hr PQ + 5 hr recovery). The bar is 10 μm.

FIGURE S3. Effects of Drp1 expression levels on aggregate formation and the effects fission mutants on growth, paraquat sensitivity and stress gene expression. (A) Effects of Paraquat on the broodsizes of wildtype, Fis1, Mff and Pink1 mutant animals. Percentages were based on the broodsizes of the different stains grown without Paraquat (mean and SD, n > 20). (B) Expression levels of heatshock and autophagy genes in Fis1 and Mff mutants relative to the average expression level in wildtype animals. Values were determined with qPCR (mean and SD, n = 3). (C) Fis1 and Mff mutants both have significantly lower broodsizes than wildtype when grown at 26°C, but the Fis1 Mff quadruple mutant is no worse, showing that there is no additive or synergistic effect (mean and SD, n=3, unpaired Student's t test). (D) Drp1 RNAi eliminates LGG-1 aggregates in the Fis1 double mutant, while ectopic overexpression of DRP-1 using a $P_{myo\text{-}3}$*::DRP-1* construct induces more aggregates in the Fis1 double mutant. The bar is 10 μm.

FIGURE S4. A small shift towards fused mitochondria in *C. elegans* with Pink1 deficiencies. (A) Examples of mitochondria in wildtype worms grown with no RNAi, with RNAi for *eat-3*, *fzo-1*, *drp-1* or *pink-1* genes, and in the *pink-1(tm1779)* deletion strain. Mitochondria were labeled with YFP::TOM70. The bar is 10 μm. (B) Quantification of the mitochondrial morphologies in panel (A). Images were classified as predominantly fragmented (F), tubular (T) or connected (C) mitochondria morphologies. In addition, cells with brightly stained abnormal mitochondria (A) and swollen mitochondria (S) were noted. Percentages for each class are shown. The experiment was double blind with a total of 300 pooled and relabeled images (n = 30 for *eat-3*, *fzo-1* and *drp-1* RNAi and 60 – 90 for the others).

FIGURE S5. LC3 aggregates are observed with alternative methods for Fis1 inhibition. (A) LC3-aggregates in HCT116 Fis-/- cells treated for 3 hr with 10 μM Valinomycin. (B) The effects of Fis1 deficiencies on Antimycin A induced clustering of LC3 can be replicated with longer incubations (9hr for HCT116 WT and Fis1-/- cells transfected with GFP-LC3 and mCherry-Parkin). The degree of clustering was classified as in Figure 5C (> 100 cells per experiment). (C) The effects of Fis1 deficiencies on Antimycin A induced clustering of LC3 can also be replicated with floxed cells (3 hr Antimycin A treatment of GFP-LC3 and Parkin transfected Fis1 flox/- and Fis1-/- cells). (D) The effects of Fis1 deficiencies on Antimycin A induced clustering of LC3 can also be replicated with Fis1 shRNA (3 hr Antimycin A treatment of HCT116 cells infected with lentivirus expressing control). (E) The

effects of Fis1 deficiencies on Antimycin A induced clustering of LC3 can be replicated with Fis1 shRNA. (F) Rescue shown by reduced clustering of LC3 in Fis1 -/ cells with Fis1 reintroduced by a transfection construct. Empty vector or pcDNA/Fis1 expression construct were transfected into Fis1-/- cells with GFP-LC3 and Parkin, followed by 3 hr incubation with Antimycin A and immunostaining with anti-Parkin and anti-Fis1 antibodies. Two examples are shown for each condition. (G) The degree of GFP-LC3 clustering was classified as in Figure 5C. (H) Parkin overexpression is essential for Antimycin A to induce LC3 aggregates in Fis1 -/- cells. HCT116 WT and Fis1-/- cells expressing GFP-LC3 were transfected with control vector or mCherry-Parkin constructs, followed by 3 hr incubation with Antimycin A. Cells were immunostained with anti-Tom20 antibody. (I) Mitochondrial morphologies in HeLa cells transfected with scrambled or Fis1 siRNA oligonucleotides followed by a 3 hr treatment with Antimycin A, PMA or STS as in Figure 9A. Images show that fission is induced to varying degrees by these treatments, but there is no noticeable difference between scrambled and Fis1 siRNA cells after this relatively long incubation. The bars are 10 μm.

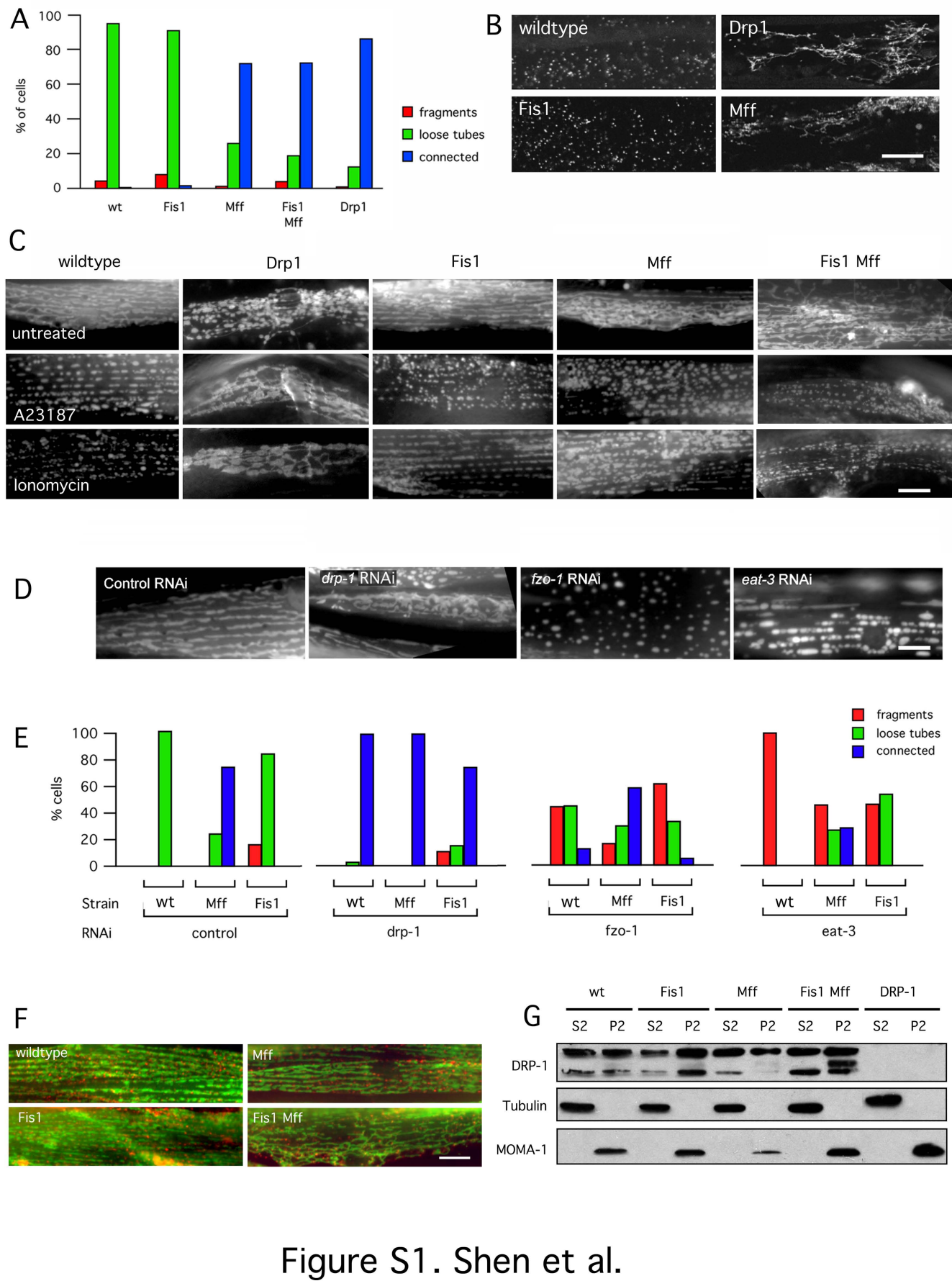

Figure S1. Shen et al.

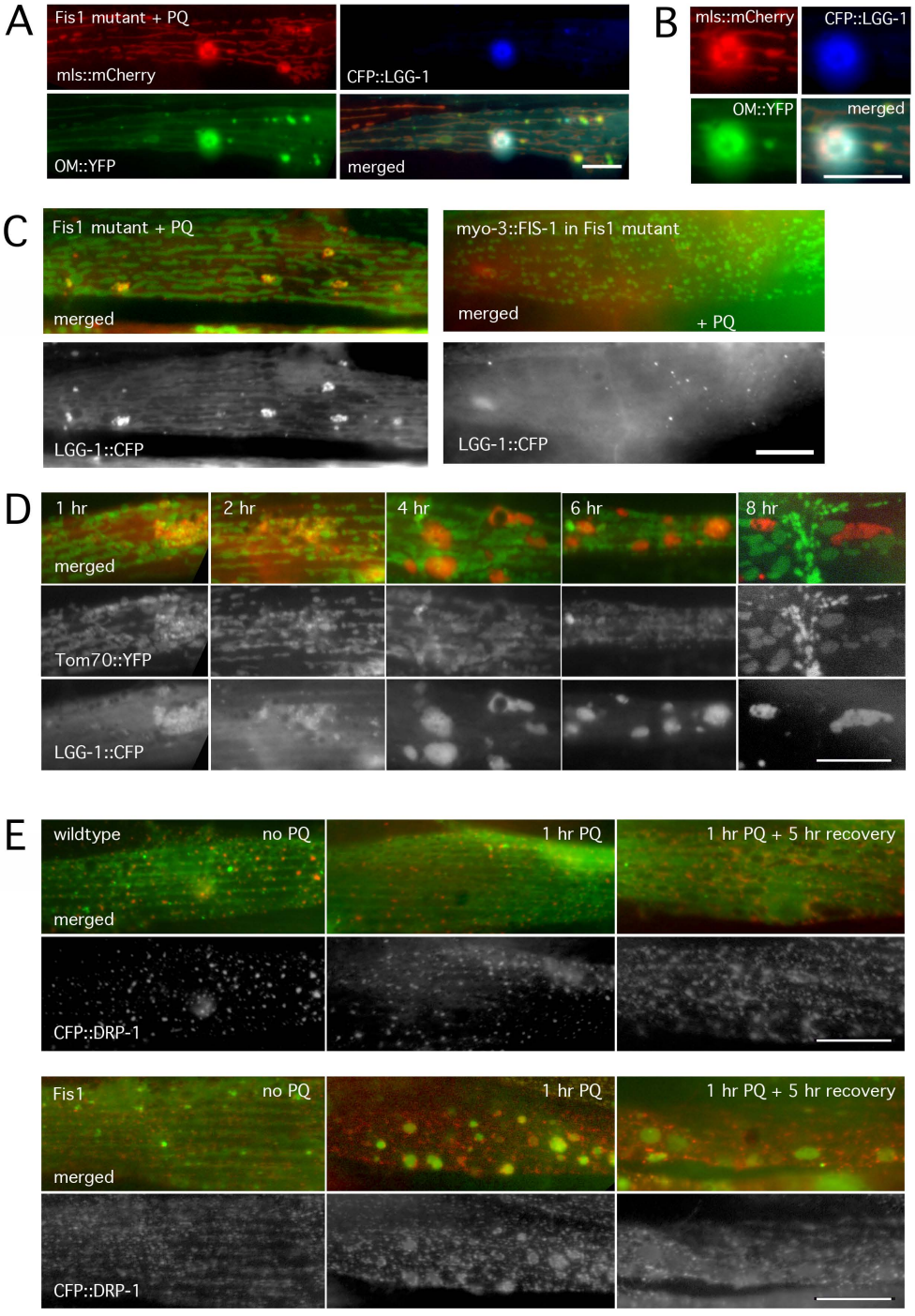

Figure S2. Shen et al.

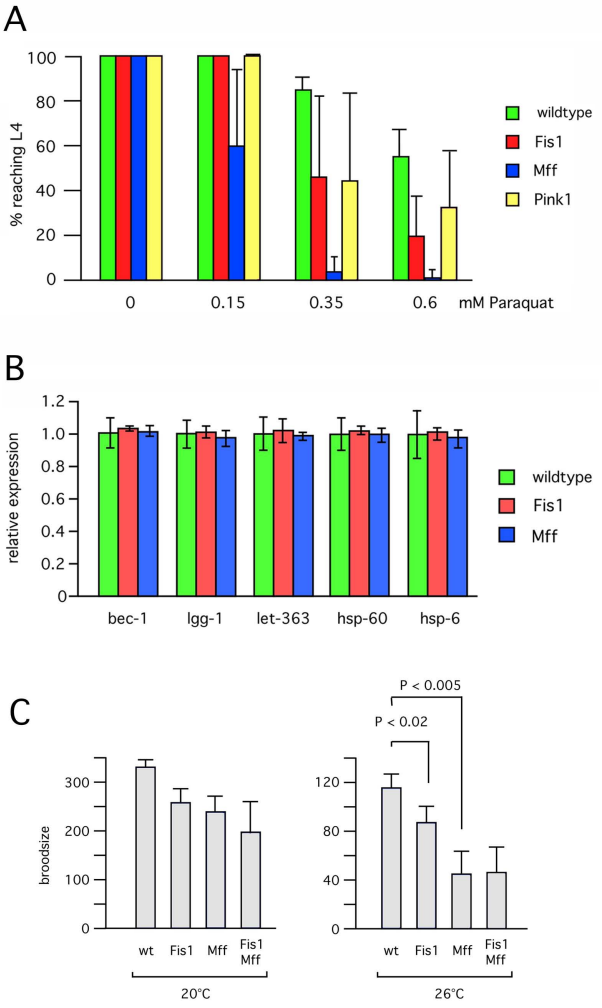

Figure S3. Shen et al.

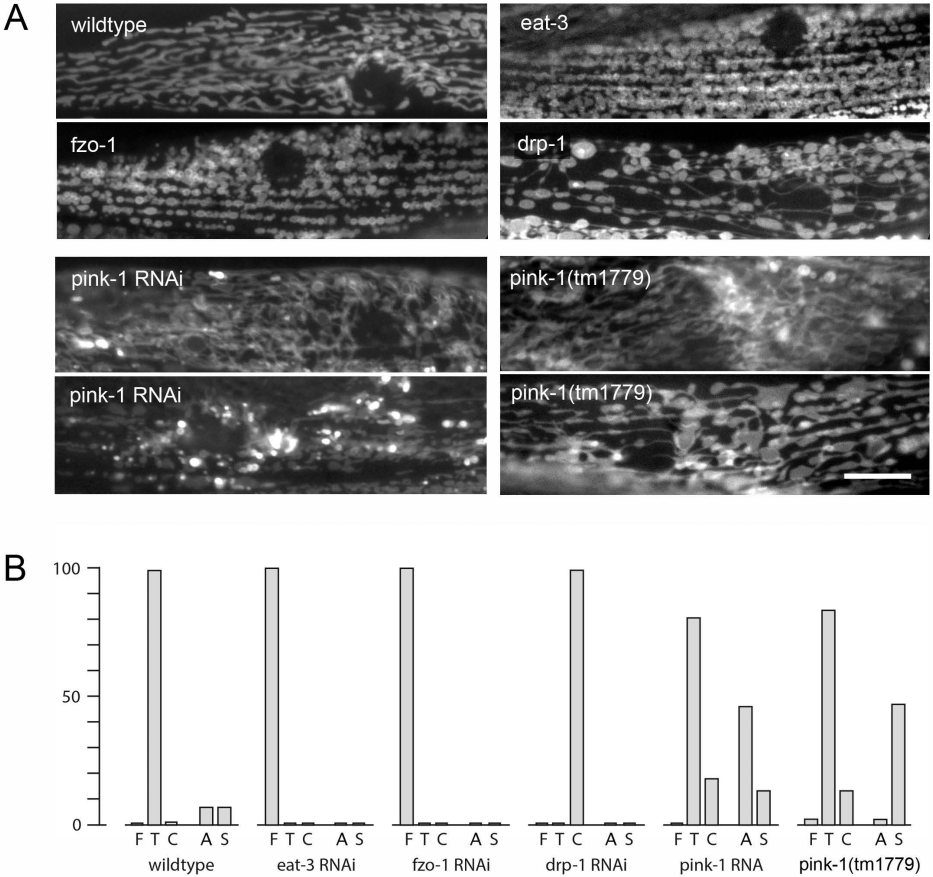

Figure S4. Shen et al.

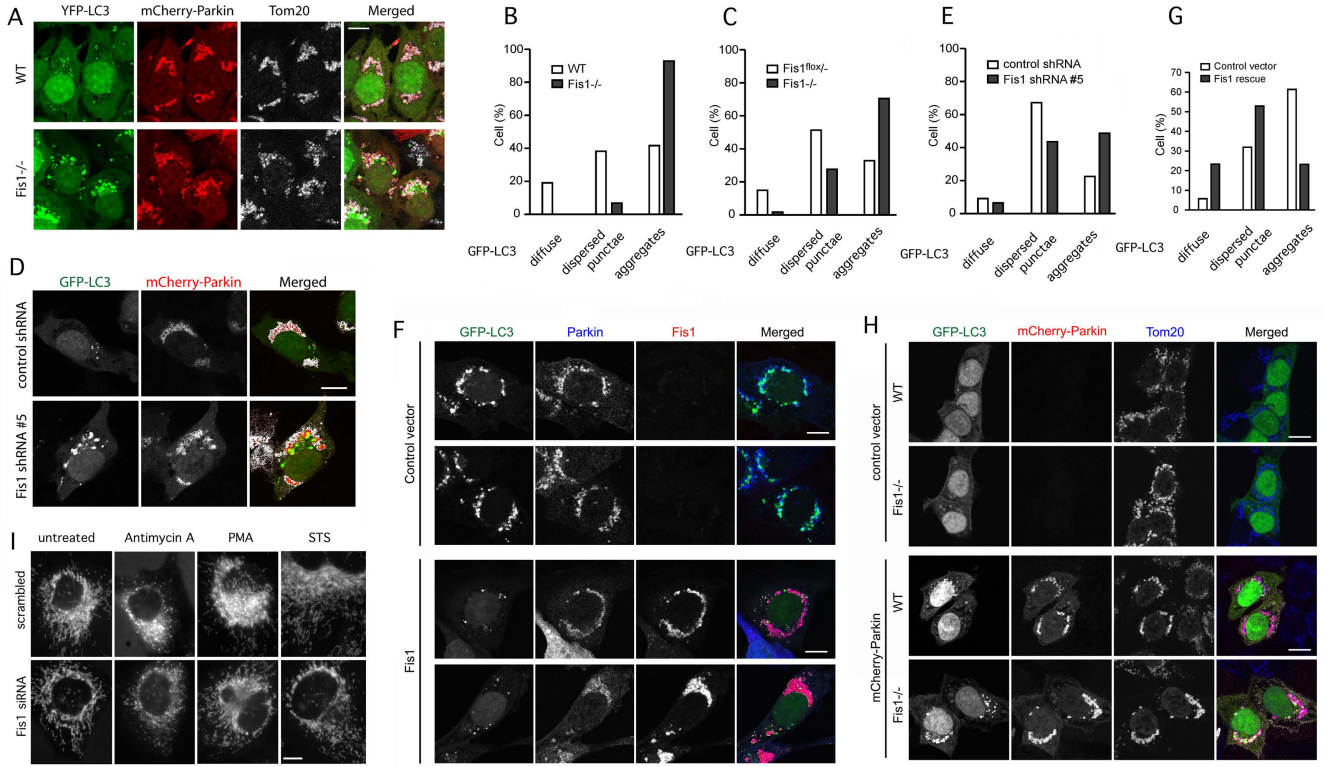

Figure S5. Shen et al.